# Environmental Behaviors of (E)-Pyriminobac-methyl in Agricultural Soils

**Wenwen Zhou**
Jiangxi Agricultural University
**Haoran Jia**
Jiangxi Agricultural University
**Lang Liu**
Jiangxi Agricultural University
**Baotong Li** ( btli666@163.com )
Jiangxi Agricultural University
**Yuqi Li**
Jiangxi Agricultural University
**Meizhu Gao**
Jiangxi Agricultural University

**Research Article**

**Keywords:** (E)-pyriminobac-methyl, adsorption–desorption, degradation, leaching, agricultural soils

**Posted Date:** July 19th, 2021

**DOI:** https://doi.org/10.21203/rs.3.rs-708755/v1

# Environmental behaviors of (*E*)-Pyriminobac-methyl in agricultural soils

Wenwen Zhou[a], Haoran Jia[b], Lang Liu[b], Baotong Li[b*], Yuqi Li[b], Meizhu Gao[b]

[a] College of Food Science and Engineering, Jiangxi Agricultural University, Nanchang 330045, China

[b] College of Land Resources and Environment, Jiangxi Agricultural University, Nanchang 330045, China

*Corresponding Author: Baotong Li, Tel.: 86-791-83813420, E-mail: libt666@163.com

**Abstract**

(*E*)-Pyriminobac-methyl (EPM), a pyrimidine benzoic acid esters herbicide, has a high potential as weedicide; nevertheless, its environmental behaviors are still not well understood. In this study, we systematically investigated for the first time the adsorption–desorption, degradation, and leaching behaviors of EPM in agricultural soils from five exemplar sites in China (characterized by different physicochemical properties) through laboratory simulation experiments. The EPM adsorption–desorption results were well fitted by the Freundlich model ($R^2$ > 0.9999). In the analyzed soils, the Freundlich adsorption (i.e., $K_{f\text{-}ads}$) and desorption (i.e., $K_{f\text{-}des}$) coefficients of EPM varied between 0.85–32.22 $mg^{1-1/n}$ $L^{1/n}$ $kg^{-1}$ and between 0.78–5.02 $mg^{1-1/n}$ $L^{1/n}$ $kg^{-1}$, respectively. Moreover, the degradation of EPM reflected first-order kinetics: its half-life ranged between 37.46–66.00 d depending on the environmental conditions, and abiotic degradation was predominant in the degradation of this compound. The mobility of EPM in the five soils varied from immobile to highly mobile. The groundwater ubiquity score ranged between 0.9765–2.7160, indicating that EPM posed threat to groundwater quality. Overall, the results of this study demonstrate the easy degradability of EPM, as well as its high adsorption affinity and low mobility in soils with abundant organic matter content and high cation exchange capacity. Under such conditions, there is a relatively low contamination risk for groundwater systems in relation to this compound. Overall, our findings provide a solid basis for predicting the environmental impacts of EPM.

**Keywords:** (*E*)-pyriminobac-methyl, adsorption–desorption, degradation, leaching, agricultural soils

## 1. Introduction

Herbicides are usually applied to chemically control the growth of weeds associated with different types of crops, both in China and worldwide (Barchanska et al. 2021; Brillas 2021). Unfortunately, with the applications of weedicides, they have been detected outside of their original application sites, meaning that they contribute to environmental contamination (Jiang et al. 2018; Perotti et al. 2020). In recent years, the groundwater pollution caused by herbicides has attracted increasing attention worldwide (Khan et al. 2020; Wu et al. 2017). Importantly, the environmental fate of herbicides in soil mainly depends on the adsorption–desorption, degradation, and leaching processes. In fact, herbicides can be transferred from soil to groundwater through surface runoff or leaching, resulting in groundwater pollution (Cueff et al. 2020; Gawel et al. 2020). Furthermore, the adsorption–desorption rate and the degradation capability of herbicides regulate the migration of herbicides: the groundwater ubiquity score (GUS) can be used to evaluate their ecological and environmental safety (Acharya et al. 2020; Liu et al. 2021). However, few scholars have assessed the effects of soil properties on the adsorption–desorption, degradation, and leaching behaviors of weedicide, especially the environmental consequences of these changes.

Pyriminobac-methyl (PM)[methyl-2-(4,6-dimethoxy-2-pyrimidinyloxy)-6-(1-methoxyiminoethyl) benzoate] (Fig. S1), is composed of a mixture of its (*E*) - isomer (I) and (*Z*) - isomer (II) as the active ingredient due to its chemical structure contain oxime(Song et al. 2010), a mixture of two isomers (I and II) in a > 9:1 (major/minor) ratio which was developed from sulfonylurea by Kumiai Chemical Industry Co., Ltd. In 1996 (Tokyo, Japan)(Tamaru and Saito 1996). Tamaru et al. (1997)) reported that (*E*) - isomer (I) has been confirmed to restrain the plant enzyme acetolactate synthase (ALS) and prevent branched chain amino acid biosynthesis, and the (*E*) - pyriminobac-methyl (EPM) showed stronger soil adsorption and weaker hydrophilic properties

than (*Z*) - pyriminobac-methyl (ZPM), thus EPM was selected as the best compound to develop a commercial weedicide, which is commonly used to control the growth of sedges and both gramineous and annual weeds. The chemistry of EPM is well understood; the octanol-water partition coefficient is 2.31 (low) at pH 7, 20 °C, the solubility - in water is 9.25 mg $L^{-1}$ (low) at 20 °C, and the vapour pressure is just $3.1\times10^{-5}$ Pa (low) at 20 °C (Lewis et al. 2016). A distinct advantage of EPM as a weedicide is that, this compound has an herbicidal activity 1.5–2 times higher and requires an application rate 1/5–1/10 lower than bensulfuron-methyl (a broad-spectrum herbicide) on *Echinochloa crusgalli* and *Leptochloa chinensis* (Iwakami et al. 2015; Shibayama 2001; Song et al. 2010). Notably, EPM can prevent the growth of *E. crusgalli* and *L. chinensis* populations and suppress them effectively over long periods, while being non-toxic, and eventually increasing the yield of paddy rice and subsequent crops (e.g., rape, cabbage, *Astragalus smicus*, wheat, and potato) (Iwafune et al. 2010; Qin et al. 2017; Tang et al. 2010; Yoshii et al. 2020). Nevertheless, few studies have lucubrated the environmental behaviors of EPM after it was widely used as herbicide in the farming industry.

Most former investigations on EPM as a weedicide mainly focused on the photo-transformation in water and low temperature storage stability in paddy rice. Inao et al. (2009)) demonstrated that the photoconversion of PM in water is the main fate, and the main process is EPM / ZPM reached approximately equilibrium after 4.5 h, furthermore, the EPM / ZPM ratio is about 1/1.35. Another researcher found that even if proper water management to prevent EPM surface runoff from paddy fields was practiced, a significant amount of EPM components were discharged into drainage channels through percolation (Sudo et al. 2018). Nevertheless, the effects of soil properties on the adsorption–desorption, degradation, and leaching behaviors of EPM have rarely been reported.

A number of researchers have reported that the soil matrix is a highly complicated system, in which environmental processes (e.g., the sorption–desorption and leaching of herbicides) are affected by multiple factors, including the soil organic matter (OM) content, pH, cation exchange capacity (CEC), microbial or chemical degradation, chemical type, environmental conditions (e.g., temperature, humidity, and rainfall), and texture (Alonso et al. 2011; Rao et al. 2020; Xie et al. 2020; Zhou et al. 2019a). Nevertheless, soil organic or inorganic colloids and pH (pH < $pK_a$ neutral state and pH > $pK_a$ negative charge) can influence soil–herbicide interactions. In this context, the leaching of anionic compounds is likely (Pérez-Lucas et al. 2020). Moreover, the leaching of herbicides in soil and the associated risk of water pollution are both affected by sorption and desorption (Xie et al. 2020).

Until present, the environmental fate of EPM in soils has not been studied in detail. Clarifying the adsorption and transport of EPM in soil is very important for the protection of surface water and groundwater from EPM pollution. Hence, this study aimed at: 1) gaining an essential understanding of the adsorption–desorption, degradation, and leaching behaviors of EPM in agricultural soils through laboratory simulation experiments; 2) determining the effects of soil properties on the above behaviors in agricultural soils; and 3) conducting a basic evaluation of the safety and applicability of EPM in the environment. Overall, our results provide a scientific basis for the prevention or, at least, minimization of the possible effects of EPM on groundwater, as well as for modeling the fate of EPM in the environment and the potentially associated risks.

## 2. Materials and Methods

### *2.1. Chemicals*

EPM (99.0%; chemical formula: $C_{17}H_{19}N_3O_6$; structure shown in Fig. S1) was obtained from ZZBIO Co., Ltd. (Shanghai, China). Moreover, we used only organic solvents of chromatographic grade (Sigma-Aldrich, Germany). EPM was dissolved in acetonitrile, obtaining a 1000 mg $L^{-1}$ test mother liquor. Moreover, a standard EPM working solution (0.01–5.00 mg $L^{-1}$) was prepared by diluting the stock solution with a $CaCl_2$ solution (0.01 mol $L^{-1}$), which was used as an electrolyte to maintain a constant ionic strength and reduce the cationic exchange.

In March 2020, five different soils were sampled from the surface layer (0–20 cm) of paddy fields located in five Chinese provinces: Phaeozem (S1, from Heilongjiang), Anthrosol (S2, from Zhejiang), Ferralsol (S3, from Jiangxi), Alisol (S4, from Hubei), and Plinthosol (S5, from Hainan). The soil samples were all air-dried, ground, and passed through a 2-mm sieve before being used. Afterward, standard soil testing methods were applied to define the basic physicochemical properties of the soils (Table S1) (Gee 1986; Jackson 1958; Nelson 1985), which were then classified based on the system of the World Reference Base for Soil Resources (WRB) (L'Huillier 1998). Interestingly, the EPM residues in the analyzed soils were always below the detection limit.

*2.2. Extraction and final analyses*

The soil samples were transferred to centrifuge tubes and 10 mL of acetonitrile (containing 0.1% of ammonia water) were added to each of them for extracting EPM. After vortexing the tubes for 5 min, we added 2 g of NaCl and 3 g of $MgSO_4$. Then, the tubes were capped and vortexed again for 1 min and centrifuged at 2,400 × g for 5 min. The supernatant (1.5 mL) was transferred into a 2.5-mL single-use centrifuge tube that was already containing the sorbent (50 mg $C_{18}$ + 150 mg $MgSO_4$). Afterward, all the samples were vortexed again for 1 min and centrifuged at 5,000 rpm for 5 min. Finally, the resulting supernatant was extracted with a sterile syringe,

passed through a 0.22-μm organic membrane filter, and poured into vials for UPLC system (1260 series, Agilent Technologies, USA) equipped with a triple quadrupole mass spectrometer (6460C series, Agilent Technologies) using positive ion mode in multiple reaction monitoring (MRM) mode analysis. The instrument parameters for Agilent 6460C QQQ UPLC-MS/MS analysis are as follows: The flow rate was maintained at 0.2 mL $min^{-1}$, and the column (Agilent ZORBAX Eclipse XDB-C18, length 150 mm, inner diameter = 4.6 mm, 5μm coating) was heated to 35°C. The mobile phase A was water which consisted of 0.1% formate and mobile phase B was acetonitrile. Gradient condition was: 0.0-0.5 min, 20% B; 0.5-1.0 min, 20%-80% B; 1.0-4.0 min, 80% B; 4.0-5.0 min, 20% B. The mass spectrometer was operated in electrospray ionization positive with MRM scanning mode, dry gas temperature at 500 °C, Ion source temperature at 150 °C, desolvation gas flow at 1000 L $h^{-1}$; capillary voltage at 2500 V; cone voltage at 18 V and collision gas was argon, dwell time at 50 ms, collision pressure at 58 eV.

The efficiency of the EPM extraction during the adsorption–desorption, degradation, and leaching experiments was evaluated based on the results of recovery experiments. The average recovery rates of EPM in the adsorption–desorption experiments, at initial spiked concentrations of 0.1 and 1.0 mg $kg^{-1}$ in the soils, varied between 94.3–102.4% (relative standard deviation (RSD) = 1.1–3.8%). Meanwhile, the average recovery rates of EPM in soil in the degradation experiments, at initial spiked concentrations of 0.01, 0.2, and 2.0 mg $kg^{-1}$ in the soils, ranged between 92.6–106.0% (RSD = 1.1–2.9%). Furthermore, the average recovery rates of EPM at initial spiked concentrations of 0.0001, 0.01, and 0.1 mg $L^{-1}$ in the supernatant of soils were 88.7–107.9% (RSD = 1.7–4.9%). Furthermore, the average recovery rates of EPM in the leaching experiments at initial spiked concentrations of 0.05 and 1.0 mg $kg^{-1}$ in the soils were 95.8–109% (RSD = 1.6–4.4%).

*2.3. Soils samples*

The batch equilibration method suggested by the GB 31270.4-2014 guidelines: Adsorption/Desorption in Soils for these soils (GB 2014b) was applied to conduct adsorption–desorption experiments. First, for the adsorption kinetics tests, each soil sample (2.0 g) was introduced in a centrifuge tube containing 10 mL of a EPM aqueous solution (1 mg $L^{-1}$). For each of these tubes, we also analyzed a blank tube (which contained no herbicide) and a control tube (which contained no soil). All the tubes were then shaken by an oscillator at 25 °C ± 1 °C for different time intervals of 0.5, 1, 2, 4, 6, 8, 12, 16, 20, and 24 h.

The desorption kinetics were analyzed instead by taking 5 mL of supernatant from each tube after adsorption equilibration and by replacing them with an equal volume of $CaCl_2$ solution (which contained no EPM). A microvortex mixer was used to thoroughly mix the resulting solution and an oscillator was used to shake it at 25 °C ± 1 °C for several time intervals: 0.5, 1, 2, 4, 6, 8, 12, and 24 h. Finally, for the high-performance liquid chromatography-mass spectrometry (UPLC-MS/MS) analyses, the samples were centrifuged for 10 min at 2,400×g and the supernatants were filtered through 0.22-μm mixed-cellulose ester filter membranes.

The adsorption–desorption equilibrium time of EPM in the five soils was 24 h (Fig. 1); moreover, the initial EPM concentrations adopted for these experiments were 0.01, 0.10, 0.50, 1.00, and 5.00 mg $L^{-1}$. The concentration of EPM in the supernatant was determined after centrifugation. Then, the amount of adsorbed–desorbed EPM in each soil was calculated based on the concentration of EPM in the solution before and after the adsorption–desorption process. The supernatant removed after the adsorption experiments was replaced with 5 mL of $CaCl_2$ containing no EPM; then, the tubes were shaken for 24 h and centrifuged. Finally, the EPM concentration was determined based on the supernatant collected after this procedure. Considering the

results of preliminary experiments and with the aim of desorbing the majority of the adsorbed EPM, we decided to repeat the desorption process for at least three times.

*2.4. Degradation experiments*

By following the GB 31270.1-2014 guidelines(GB 2014a), we performed a series of EPM soil degradation experiments. To ensure aerobic conditions, 20 g of each type of agricultural soil were weighed and introduced in 250-mL Erlenmeyer flasks (in three replicates). Ultrapure water was added during the subsequent cultivation process in order to maintain the soil water content at 60% of the maximum water holding capacity. We then spiked each soil sample with 400 μL of the 100 mg $L^{-1}$ EPM working solution (achieving an initial concentration of 2 mg $kg^{-1}$ in the soil: the water-soluble, organic solvent volume was ≤1%) and then cultured in the dark in an incubator kept at 25 ± 1 °C. Subsequently, we collected three parallel sub-samples on 0, 1, 2, 4, 6, 10, 15, 30, 45, 60, 90, and 120 day, and the EPM content was determined by UPLC-MS/MS on the respective days of collection. The amount of water in the Erlenmeyer flasks was periodically adjusted during the culturing process with the aim of retaining the original water-holding state. Each treatment was done in triplicate, totalizing 60 samples per treatment (5 soil samples per treatment per sampling day; 12 sampling days in total), The following experiment was done in the same way.

Another set of experiments was conducted under anaerobic conditions. In this case, we first cultured the soil samples for 30 days and then added a 2 cm-thick water layer to each of them. To maintain the desired conditions, $N_2$ was continuously introduced into the culture system. The soil samples were subsequently moved into an incubator and cultivated in the dark at 25 ± 1 °C. Finally, three parallel sub-samples were collected on 0, 1, 2, 4, 6, 10, 15, 30, 45, 60, 90, and 120 day, and the EPM content was determined by UPLC-MS/MS on the respective days of collection.

A set of degradation experiments was performed under sterilized conditions. With this objective, the sterilized soils (20 g each) were weighed and introduced in 250-mL Erlenmeyer flasks in three replicates. Notably, in order to keep the soil water content at 60% of the maximum water holding capacity, sterile water was added during the cultivation process. Then, each soil sample was spiked with 400 μL of the 100 mg $L^{-1}$ EPM working solution, achieving an initial concentration of 2 mg $kg^{-1}$ (the water-soluble, organic solvent volume was ≤1%). The samples were hence moved into an incubator and cultured in the dark at 25 ± 1 °C. Three parallel sub-samples were collected on 0, 1, 2, 4, 6, 10, 15, 30, 45, 60, 90, and 120 day, and the EPM content was determined by UPLC-MS/MS on the respective days of collection.

These experiments were done under different soil moisture conditions and aerobic conditions, at a EPM fortification level of 2 mg $kg^{-1}$. After adjusting their moisture by adding water (water percentage = 40%, 60%, and 80% of the total volume), the soils were incubated in the dark at 25 ± 11 °C. During this last phase, we regularly added ultrapure water to keep the moisture at 40%, 60%, and 80%.

*2.5. Leaching experiments*

The herbicide leaching process was investigated by following the GB 31270.5-2014 guidelines (GB 2014c). PVC columns (length = 35 cm, internal diameter = 4.5 cm), each hand-packed with 600–800 g of one soil type, were used to observe the downward movement of the herbicide. Notably, the top 3 cm and the bottom 2 cm were filled with quartz sand (for minimizing soil disturbance) and glass wool + sea sand (for avoiding soil loss). After packing each column, we removed any air still present in the column by adding 0.01 mol $L^{-1}$ $CaCl_2$; moreover, the excess water was eliminated by gravity. The pore volume (PV) was determined by subtracting the volume of water leached from that of the water added. Subsequently, 1 mL of acetonitrile solution containing 200 μg $mL^{-1}$ of the herbicide (spiking level = 1 μg $g^{-1}$) was added to the top of each column. afterward, the

adsorption equilibrium was achieved by infiltrating 700 μL of 100 mg $L^{-1}$ EPM solution into soil surface and leaving it to rest for 24 h. To simulate rainfall leaching, 2,000 mL of 0.01 mol $L^{-1}$ $CaCl_2$ solution (21 mL $h^{-1}$) were added into the soil column at a peristaltic pump speed of 250 mL 12 $h^{-1}$. The leachate was collected every 8 h with a conical flask. Subsequently, each soil column was extracted, cut into three parts (length = 10 cm), and analyzed by UPLC-MS/MS on the same day. The total mass of the leachate and soil fractions along the soil column was determined, together with the EPM and water contents within each of them.

*2.6. Data analysis*

The relationship between the concentrations of EPM sorbed in the soil and in the aqueous solution during the sorption–desorption equilibrium was described through the linear [Eq. (1)] and Freundlich [Eq. (2)] models (Azizian et al. 2007; Yang et al. 2021):

$$\text{Linear model: } C_s = KC_e + C \quad (1)$$

$$\text{Freundlich model: } C_s = K_f C_e^{1/n} \quad (2)$$

where $C_s$ (mg $kg^{-1}$) indicates the adsorption of EPM in the soil, $C_e$ (mg $L^{-1}$) the EPM concentration in the solution during the adsorption equilibrium, C (mg $kg^{-1}$) the amount of soil adsorption when the EPM concentration was 0 during the adsorption equilibrium, $K$ (mL $g^{-1}$) and $K_f$ ($mg^{1-1/n}$ $L^{1/n}$ $kg^{-1}$) the adsorption–desorption constants of the linear and Freundlich models, respectively ($K_{f\text{-}ads}$/$K_{f\text{-}des}$ in the adsorption–desorption process), and 1/n the adsorption empirical constant (which provides information about the non-uniformity of the adsorbent surface).

For the isothermal sorption tests, the amount of EPM adsorbed in the soil was estimated using the subtractive method [Eq. (3)]:

$$C_s = \frac{(C_0 - C_e) \times V}{m} \quad (3)$$

where $C_0$ (mg $L^{-1}$) is the amount of soil adsorption when the concentration of EPM was 0 during the adsorption equilibrium, m the soil mass (2.0 g), and *V* the solution volume (10 mL).

The amount of EPM retained by the soil after desorption was obtained instead by using [Eq. (4)], while the hysteresis index (*H*) was estimated by applying [Eq. (5)] (Fan et al. 2021; Zhang et al. 2020b):

$$C_{sj} = \frac{C_0 \times V}{m} - \frac{C_{ej} \times V}{2m} - \frac{V}{m} \sum_{n=1}^{j} C_e(j-1) \quad (4)$$

$$H = \frac{1/n_{des}}{1/n_{ads}} \quad (5)$$

where $C_{sj}$ (mg $kg^{-1}$) is the concentration of EPM adsorbed by the soil after the j-th desorption (i = 1–5), $C_{ej}$ (mg $L^{-1}$) the EPM concentration in the supernatant after the j-th desorption, *H* the hysteresis coefficient, and $1/n_{ads}$ and $1/n_{des}$ the empirical adsorption and desorption constants, respectively.

The distribution coefficient ($K_d$) was calculated based on the distribution ratio of EPM in the water–soil system by using [Eq. (6)] (Carballa et al. 2008; Ternes et al. 2004):

$$K_d = \frac{C_s}{C_e} \quad (6)$$

The sorption constants of the OC ($K_{OC}$) and OM ($K_{OM}$) contents were calculated through [Eqs. (7) and (8)] (Rae et al. 1998; Zhang et al. 2011), respectively. Moreover, the Gibbs free energy change of sorption ($\Delta G$, kJ $mol^{-1}$) (Jia et al. 2019) and the GUS (Gustafson 1989) were calculated as follows:

$$K_{OM} = 100 \times K_{f-ads} / OM\% \quad (7)$$

$$K_{OC} = 100 \times K_d / OC\% \quad (8)$$

$$\Delta G = -RT \ln K_{OM} / 1000 \quad (9)$$

$$GUS = \lg t_{1/2} \times (4 - \lg K_{OC}) \quad (10)$$

where *OM* % and *OC* % represent the soil OM and OC contents, respectively, *R* the molar gas constant (8.314 J $K^{-1}$ $mol^{-1}$), *T* (K) the absolute temperature, and $t_{1/2}$ the half-life (in days) given by [Eq. (12)]. Organic contaminants were categorized into five types: highly adsorbed compounds ($K_{OC}$ > 20,000), sub-highly adsorbed compounds (5,000 < $K_{OC}$ ≤ 20,000), medium-adsorbed compounds (1,000 < $K_{OC}$ ≤ 5,000), sub-difficultly adsorbed compounds (200 < $K_{OC}$ ≤ 1,000), and difficultly adsorbed compounds ($K_{OC}$ ≤ 200)(GB 2014b).

The degradation data relative to herbicides in soil could be successfully fitted to a first-order kinetic model [Eq. (11)], previously used in similar studies (Bailey et al. 1968; Liu et al. 2021; Ou et al. 2020):

$$C_t = C_0 e^{-kt} \quad (11)$$

where $C_t$ (mg $kg^{-1}$) and $C_0$ (mg $kg^{-1}$) are the concentrations of EPM in the soil at incubation times t (d) and 0 (d), respectively, while *k* is the first-order rate constant ($d^{-1}$).

The half-life ($t_{1/2}$) to be used in above model was calculated through [Eq. (12)] (Yin and Zelenay 2018):

$$t_{1/2} = 0.693/k \quad (12)$$

Four categories of herbicide degradability were defined: easily degradable ($t_{1/2}$ ≤ 30), moderately degradable (30 < $t_{1/2}$ ≤ 90), slightly degradable (90 < $t_{1/2}$ ≤ 180), and poorly degradable ($t_{1/2}$ > 180)(GB 2014a).

Based on the content of EPM in different sections of the soil columns and in the leachate [Eq. (13)](GB 2014c), we were able to calculate the leaching rate of EPM:

$$R_i = \frac{m_i}{m_0} \times 100 \quad (13)$$

where $R_i$ (%) is the ratio of EPM content in each soil section or in the leachate to the total added amount, $m_i$ (mg) the mass of EPM in each soil section (where $i$ = 1, 2, 3, and 4, representing the 0–10 cm, 10–20 cm, and 20–30 cm soil sections and in the leachate, respectively), and $m_0$ (mg) the total added amount of EPM ($m_0$ = 0.02 mg). Regarding the mobility scheme we defined the following $R_i$ ranges: class 1 (immobile, $R_1 > 50$ %), class 2 (slightly mobile, $R_2 + R_3 + R_4 > 50$ %), class 3 (mobile, $R_3 + R_4 > 50$ %), and class 4 (highly mobile, $R_4 > 50$ %)(GB 2014c).

The data fittings (to the linear and Freundlich models for the adsorption isotherms and to the simple first-order kinetic model for degradation) were conducted with OriginPro 8.05 (OriginLab Corp., Northampton, USA). All the values reported here were calculated as the means of three replicates; furthermore, the differences between these means were statistically analyzed through Duncan's multiple range test, while their reciprocal relationships were determined though a Spearman's correlation analysis using SPSS Statistics 22.0 (IBM SPSS, Somers, USA).

## 3. Results and discussion

### *3.1. Adsorption–desorption kinetics*

The adsorption and desorption kinetic curves of EPM in different types of agricultural soils are shown in Fig. 1. After EPM had been in contact with the soil solution for 1 h, the concentration of EPM exhibited a sharp drop (from 0 to 95.35, 75.45, 51.57, 77.41 and finally 65.84 % between S1–S5). This event corresponded to the fast sorption phase. After 2–8 h, the EPM soil system entered the slow adsorption stage and there was a gradual increase in the sorption of EPM. This last process reached an equilibrium state of EPM sorption after 8 h, which

was reflected by stable concentrations of EPM. The sorption of EPM decreased from the Phaeozem (S1, 97.99%) to the Anthrosol (S2, 79.69%), Alisol (S4, 77.81%), Plinthosol (S5, 72.57%), and Ferralsol (S3, 52.35%) (Fig. 1a). This trend reflected the soils' OM contents. Previous studies have also found that the sorption of organic chemicals in soils is mainly related to their OM contents (Xu et al. 2021; Zhou et al. 2019b).

The desorption equilibration of EPM in soil was slightly slower and a hysteresis effect was observed. The rapid and slow desorption stages occurred between 0–2 h and 2–12 h, respectively; afterward, the concentration of EPM remained unchanged, until the desorption process reached its equilibrium state (within 24 h). Based on these data, we defined 24 h as the period of EPM adsorption-desorption. The desorption value of EPM observed in our experiments after 24 h increased from the Phaeozem (S1, 8.04%) to the Anthrosol (S2, 12.07%), Alisol (S4, 14.48%), Plinthosol (S5, 17.55%), and Ferralsol (S3, 24.08%) (Fig. 1b).

The sorption of OM in soil typically occurs during the rapid reaction and slow equilibrium phases (Calvet 1989). Therefore, the reduction of the EPM content in the solution before and after the experiment was likely due to soil sorption. According to the above results, the soil sorption rate was inversely proportional to the soil desorption rate toward EPM.

*3.2. Adsorption–desorption isotherms*

Non-linear adsorption–desorption isotherms of EPM were observed (Fig. 1). When the concentration of EPM was low, this compound was preferentially adsorbed by OM (which has a strong adsorption capacity); meanwhile, soils with higher OM contents (e.g., Phaeozems, S1) desorbed EPM slowly. The positive relationship between sorption and OM has been reported previously (Hochman et al. 2021; Obregón Alvarez et al. 2021; Patel et al. 2021). Moreover, the adsorption ability of EPM has been found to be high,

similar to those of other herbicides (e.g., chlorsulfuron, imazamethabenz-methyl, flumetsulam, and bispyribac-sodium) (Kalsi and Kaur 2019; Medo et al. 2020; Spadotto et al. 2020). Generally, a low mobility of herbicides in soil is related to a high sorption constant. Hence, the EPM contained in the soils tested in this study (excluding the phaeozem, S1) is likely to have been polluting the groundwater and surface water of the respective areas of origin.

OM adsorption in soil is currently explained mainly by partitioning and adsorption-site theories (Martins and Mermoud 1998), which are well described by the linear and Freundlich isotherm models, respectively. Our isothermal sorption and desorption data were thus fitted to these two models: the obtained fitting parameters are listed in Table 1. The average $R^2$ value for the linear model (0.9950) was smaller than that for the Freundlich model (0.9999); moreover, the $C$ values obtained for the Plinthosol (S5, –0.01 ± 0.06) by fitting the data to the linear model were negative (Table 1) and did not meet the experimental requirements, indicating that this type of model was not suitable for this experiment. Meanwhile, the sorption-site theory was found to more accurately describe the sorption–desorption process: the Freundlich model provided a more accurate description of the EPM sorption-desorption characteristics observed in this study.

Generally, larger $K_{f\text{-}ads}$ values correspond to higher sorption capacities (Carneiro et al. 2020; Khorram et al. 2018; Silva et al. 2019). Here, the $K_{f\text{-}ads}$ values of EPM ranged between 0.85 (in S4) and 32.22 (in S1) ($mg^{1-1/n}$ $L^{1/n}$ $kg^{-1}$), while the $1/n_{f\text{-}ads}$ values ranged between 0.80 (S1) and 1.06 (S5) (Table 1). In brief, S5 showed an S-type adsorption isotherm (since $1/n_{f\text{-}ads} > 1$), while S1, S2, S3, and S4 showed an L-type adsorption isotherm (since $1/n_{f\text{-}ads} < 1$). In this study, the $H$ values of EPM ranged between 0.013 (Phaeozem, S1) and 0.845 (Ferralsol, S3). Since the $H$ values were < 0.7 in S1, S2, S4, and S5, these particular soils showed a positive hysteresis: the desorption rate of EPM was lower than its sorption rate. Meanwhile, since the $H$ values in S3

were between 0.7–1.0, the sorption and desorption rates were in equilibrium: S3 did not exhibit any obvious hysteresis. Similar results were reported that hysteresis was absent when $0.7 < H < 1$(Barriuso et al. 1994; Gao and Jiang 2010; Yue et al. 2017).

Soil physicochemical properties are important factors influencing herbicide adsorption behaviors (Urach Ferreira et al. 2020; Wei et al. 2020). We determined the relationship between the Freundlich adsorption–desorption constant and the soil physicochemical (soil pH, CEC, soil clay content, OM content, and OC content) properties and carried out a linear correlation analysis based on the experimental data fitting (Table S2). The results showed that the soil pH, CEC, soil clay content, OM content, and OC content were positively correlated with $K_{f\text{-}des}$ and $K_{f\text{-}ads}$ (slope > 0). In soils, some polar contents, ionizable groups, and the CEC tend to increase during OM humification (Calvet 1989; Meimaroglou and Mouzakis 2019; Rae et al. 1998). This mechanism possibly explains the adsorption of EPM in soils high in OM and CEC. Our findings agree with those of Acharya et al. (2020)) and García-Delgado et al. (2020)): the soil humic acid and clay fractions (high in OM and CEC and possessing a high number of active sites) are capable of intense EPM adsorption; in contrast, the soil coarse sand fraction (low in OM and CEC) is characterized by a weaker EPM adsorption. Notably, the soil with the highest fumigant adsorption capacity was also possibly that with the highest OM abundance and CEC. For example, strong linear and positive correlations have been found between the adsorption–desorption of benzobicyclon hydrolysate and the soil clay content, OC content, OM content, and CEC, while moderate linear and negative correlations were observed between those processes and the soil pH (Rao et al. 2020).

The $K_{OC}$ value is typically used to indicate the EPM sorption capacity of a soil (FAO 2000; Xiang 2019) (see Table 2). EPM was sub-difficultly adsorbed in S2, S3, S4, and S5: this aspect was reflected by the $K_{OC}$ values, which ranged between 200–1,000. However, in S1 the $K_{OC}$ values ranged between 1,000–5,000,

indicating a medium adsorbance of EPM in this soil. Overall, an increasing trend in the mobility of EPM was observed from the Phaeozem (S1) to the Anthrosol (S2), Alisol (S4), Plinthosol (S5), and Ferralsol (S3). We hence infer that a relatively low soil adsorption capacity is linked to a relatively high mobility of EPM in that soil.

The degree of spontaneity of the adsorption process can be quantitatively evaluated based on variations in the $\Delta G$ values: negative $\Delta G$ values generally indicate that an adsorption process is spontaneous and exothermic (Nandi et al. 2009). Notably, the change of free energy linked to physical adsorption is smaller than that linked to chemisorption. The former is in the range of −20 to 0 kJ $mol^{-1}$, while the latter is in the range of −80 to −400 kJ $mol^{-1}$ (Bulut and Aydın 2006; Yu et al. 2004). We found that the $\Delta G$ values relative to EPM adsorption in all soils were comprised between −16.2242 and −12.5753 kJ $mol^{-1}$. Therefore, the adsorptions we observed in our experiments can be regarded as typically spontaneous and exothermic physical adsorptions (Table 2).

*3.3. Degradation of EPM in soil*

To investigate the effects of aerobic and anaerobic microorganisms on EPM degradation, we sterilized the soil samples or removed all aerobic microorganisms. The soil samples were kept in the dark at 25 ℃, maintaining a soil moisture of 60%. The degradation kinetics of EPM under aerobic, anaerobic, and sterilized conditions are depicted in Fig. 2, while the fitted parameters are summarized in Table 3. The $R^2$ values for EPM in the five soils ranged between 0.9313–0.9924, suggesting that the first-order kinetic model agreed with the correspondent degradation data. The half-life of EPM ranged between 37.46–58.25 d in the aerobic soils, between 41.75–59.74 d in the anaerobic soils, and between 60.87–66.00 d in the sterilized soils. A moderate degradation (30 d < $t_{1/2}$ ≤ 90 d) of EPM was observed under aerobic, anaerobic, and sterilized conditions. These results can be partly explained by aerobic and anaerobic transformations occurring in the soils, which have been

described by the GB 31270.1-2014 guidelines for the testing of chemicals(GB 2014a). Overall, the half-life of EPM decreased from the aerobic to the anaerobic and sterilized soils. Understanding the degradation kinetics of herbicides is critical for predicting their persistence in soil and the soil parameters, which affect regional agronomic and environmental practices (Buerge et al. 2019; Buttiglieri et al. 2009). Under dark conditions, the degradation of herbicides in soil mainly results from microbial and abiotic degradation (Marín-Benito et al. 2019). In this study, when EPM was retained under dark conditions for 30 d, its degradation rates in all soils under sterilized conditions (35.44, 36.27, 33.27, 32.80, and 34.78%) were a little slower than under anaerobic (48.60, 41.51, 35.92, 35.61, and 38.07%) and aerobic conditions (53.32, 43.20, 36.73, 35.61, and 39.31%) (Fig. 2). As the degradation rate increased only by 10% compared to that observed under sterilized conditions, degradation under aerobic/anaerobic conditions appeared to be mainly abiotic degradation. In contrast, other studies have found that anaerobic microorganisms are predominant contributors in the degradation process and capable of accelerating it. For example, the degradation rates of phenazine-1-carboxamide (PCN) were much higher under anaerobic than aerobic conditions, due to its own structural characteristics (Ou et al. 2020). Between 30–120 d, there were no significant differences in the degradation rates of EPM between sterilized and unsterilized soils, suggesting that EPM degradation was largely abiotic in this time interval. This might be attributed to a low bioavailability of EPM for microbial degradation, derived from a high adsorption affinity of this compound under the right OM content and pH conditions (Liu et al. 2021; Wang et al. 2020a). Overall, it appears that EPM decomposition in the tested soils was mainly driven by abiotic degradation.

The degradation rate of EPM decreased from S1 to S2, S4, S5, and S3 under both aerobic and anaerobic conditions (Table 3). A negative correlation was noted between the half-life of EPM and the soil OM content and CEC under aerobic conditions (slope < 0, P < 0.05; $R^2$ = 0.9478 and 0.8022, respectively); besides, a

negative correlation was observed between the half-life of EPM and the soil OM content under aerobic conditions (slope < 0, P < 0.05, $R^2$ = 0.8983). Notably, an abundance of OM and high CEC result in an increase of the carbon sources accessible to microorganisms, effectively stimulating their activity (Xu et al. 2020). In the presence of microorganisms, the particularly high OM and CEC characterizing S1, resulted in the fastest EPM degradation among those observed in all soils under aerobic and anaerobic conditions. However, under sterilized conditions, the degradation rate of EPM decreased from S2 to S4, S1, S5, and S3 (Table 3); moreover, the half-life of EPM and the soil pH exhibited a negative correlation under these same conditions (slope < 0, P < 0.05, $R^2$ = 0.8850; Table S3). The rate of EPM hydrolysis is known to be positively affected by alkaline soil pH. This relationship explains why, in the presence of elevated hydrolysis and under sterilized conditions, the fastest degradation behavior among all the tested soils was observed in S2 (which was characterized by the highest pH). Notably, the highest differences in the degradation rate of EPM were observed under aerobic conditions. In order to comprehensively evaluate the influence of various factors on this degradation rate, we hence focused on the analysis of data collected under aerobic conditions.

The data regarding the degradation behavior of EPM in the tested soils (Table 4 and Fig. 2) conform to first-order kinetics ($R^2$ > 0.8769). The half-life of EPM varied depending on the moisture conditions: it diminished from soils with a 60% moisture to those with moisture of 80% and 40%. Additionally, after 120 days, the degradation rates of EPM in soils with a 40% moisture (74.59, 73.93, 69.98, 73.21, and 71.25 for S1–S5, respectively) were obviously lower than those in soils with 80% (77.55, 75.38, 72.79, 75.44, and 73.62 for S1–S5, respectively) and 60% (80.04, 77.31, 75.43, 77.78, and 75.77% for S1–S5, respectively) moistures (Table 4 and Fig. 2d, e). These results show that, when the soil moisture increased from 40% to 60%, the decay rate of EPM accelerated, possibly due to the stimulation of a degradation pathway (e.g., through aerobic

microorganisms and chemical hydrolysis) linked to the increase in soil moisture (Liu et al. 2021; Wang et al. 2014). Conversely, EPM showed a slower decay when the soil moisture increased from 60% to 80%. This phenomenon might have been caused by an increase in sorption, which would have made EPM less bioavailable. This effect was more or less important according to the predominance of different biotic pathways of degradation (Bento et al. 2016; García-Valcárcel and Tadeo 1999).

### *3.4. Leaching potential*

In the current study, leaching experiments were performed by using soil columns, with the aim of simulating the migration of EPM in several agricultural soils. The correspondent results are shown in Fig. 3. It was found that the fluidity of EPM was lower in $S_1$ than in $S_2$, $S_3$, $S_4$, or $S_5$. Furthermore, the $R_i$ values of this compound in $S_1$, $S_2$, $S_3$, $S_4$, and $S_5$ were $R_1 = 99$ %, $R_2 + R_3 + R_4 = 55.5$ %, $R_4 = 71.95$ %, $R_2 + R_3 + R_4 = 76$ %, and $R_2 + R_3 + R_4 = 74$ %, respectively. Based on the Test guidelines on environmental safety assessment for chemical pesticide-Part 5: Leaching in soil(GB 2014c), the mobility of EPM in the soils S1–S5 was categorized as immobile, slightly mobile, highly mobile, slightly mobile, and slightly mobile, respectively. The soil OM content was found to be the most important soil property influencing the mobility of molecular herbicides, followed by the clay content and the CEC. A lower clay content is usually associated with a higher sand content, a higher proportion of large pores, a smaller specific surface area per soil unit volume, and a lower adsorption affinity for herbicides, which, overall, result in a greater herbicide mobility (Boyd et al. 1988; de Matos et al. 2001; Kulshrestha et al. 2004; Temminghoff et al. 1997). We found that a lower soil OM content corresponded to a weaker adsorption affinity, a weaker tendency of EPM to pass from the soil solution to the solid phase, a higher availability of EPM for leaching, and a stronger mobility of this same compound. Notably, the OM content increased from the Ferralsol (S3) to the Plinthosol (S5), Alisol (S4), Anthrosol (S2), and Phaeozems

(S1), while the mobility of EPM increased from the Phaeozem (S1) to the Anthrosol (S2), Alisol (S4), Plinthosol (S5), and Ferralsol (S3). This mobility tendency is the opposite compared to the adsorption affinity tendency of EPM in the five soils. As a matter of fact, it is generally known that the mobility of EPM in soil increases as its adsorption affinity decreases. Similar conclusions were reached through the study of other herbicides (Acharya et al. 2020; Zhang et al. 2020a).

Here, the GUS was also used to estimate both the leaching potential of chemicals and the risk of contaminants into groundwater. The GUS values of EPM in S1, S2, S3, S4, and S5 were 0.9765, 2.0402, 2.7160, 2.3755, and 2.6765, respectively (Table 2). The GUS value in S1 was considerably lower than 1.8, EPM should have little leaching potential in this soil (Gustafson 1989; Wang et al. 2020b); meanwhile, since the GUS values in the S2, S3, S4, and S5 soils were between 1.8–2.8, EPM has a considerable leaching potential there and, possibly, the ability to pollute groundwater (Huang 2019; Martins et al. 2018). Overall, we can infer that the risk of groundwater contamination by EPM is low in Phaeozem (S1), due to the low mobility of this compound; however, the risk is much higher when the same compound is contained in Anthrosol (S2), Ferralsol (S3), Alisol (S4), and Plinthosol (S5).

## 4. Conclusions

In this study, we found that EPM degrades easily, has a high adsorption affinity and a low mobility in Phaeozem (S1), which result in a low contamination risk for groundwater systems. On the contrary, this compound degrades slowly in Anthrosol (S2), Ferralsol (S3), Alisol (S4), and Plinthosol (S5), due to a low adsorption affinity and moderate mobility, which result in a high contamination risk for groundwater systems. The adsorption–desorption, degradation, and leaching of EPM were systematically explored in five agricultural soils. We noticed that physical adsorption was the main mode of EPM adsorption. The effects of soil physicochemical

properties on the adsorption and desorption of this compound were quantified by linear regression analysis. In this regard, the Freundlich adsorption ($K_{f\text{-}ads}$) and desorption ($K_{f\text{-}des}$) constants were linearly and positively correlated with the soil OC content, OM content, and CEC, while nonsignificant correlations were observed among the above constants and the soil pH and clay content.

The dissipation of EPM depended mainly on soil conditions (i.e., moisture, pH, and soil type). EPM degradation was most likely derived from abiotic degradation mechanisms; furthermore, the leaching ability of EPM increased from the Phaeozem (S1) to the Anthrosol (S2), Alisol (S4), Plinthosol (S5), and Ferralsol (S3). Overall, the high leaching ability and desorption capacity of EPM were accompanied by a low adsorption capacity and there were no significant relationships between pH and the leaching rate of EPM in the five types of soils. In contrast, the OM content, CEC, and soil clay content were the main responsible for the observed leaching rates.

To completely understand the fate of EPM in the environment, it is necessary to perform additional studies on the microbial community structures and functional diversities of other types of soil besides those analyzed here. As a matter of fact, there are still only a few studies on the environmental fate of EPM; therefore, our results may serve as a reference for evaluating the risks involved in the increasingly wide application of this compound.

## Declaration of Competing Interest

The authors declare that they have no known competing financial interests or personal relationships that could have appeared to influence the work reported in this paper.

## Acknowledgements

This work is financially supported by the National Key Research and Development Plan of China (2017YFD0301604).

## References

Acharya SP, Johnson J, Weidhaas J (2020) Adsorption kinetics of the herbicide safeners, benoxacor and furilazole, to activated carbon and agricultural soils. Journal of Environmental Sciences 89:23-34 doi:https://doi.org/10.1016/j.jes.2019.09.022

Alonso DG, Koskinen WC, Oliveira RS, Constantin J, Mislankar S (2011) Sorption–Desorption of Indaziflam in Selected Agricultural Soils. J Agric Food Chem 59(24):13096-13101 doi:10.1021/jf203014g

Azizian S, Haerifar M, Basiri-Parsa J (2007) Extended geometric method: A simple approach to derive adsorption rate constants of Langmuir–Freundlich kinetics. Chemosphere 68(11):2040-2046 doi:https://doi.org/10.1016/j.chemosphere.2007.02.042

Bailey GW, White JL, Rothberg T (1968) Adsorption of Organic Herbicides by Montmorillonite: Role of pH and Chemical Character of Adsorbate. 32(2):222-234 doi:https://doi.org/10.2136/sssaj1968.03615995003200020021x

Barchanska H, Tang J, Fang X, Danek M, Płonka J, Sajdak M (2021) Profiling and fingerprinting strategies to assess exposure of edible plants to herbicides. Food Chemistry 335:127658 doi:https://doi.org/10.1016/j.foodchem.2020.127658

Barriuso E, Laird D, Koskinen W, Dowdy R (1994) Atrazine Desorption From Smectites. Soil Science Society of America Journal - SSSAJ 58 doi:10.2136/sssaj1994.03615995005800060008x

Bento CPM, Yang X, Gort G, et al. (2016) Persistence of glyphosate and aminomethylphosphonic acid in loess soil under different combinations of temperature, soil moisture and light/darkness. Science of The Total Environment 572:301-311 doi:https://doi.org/10.1016/j.scitotenv.2016.07.215

Boyd SA, Lee J-F, Mortland MM (1988) Attenuating organic contaminant mobility by soil modification. Nature 333(6171):345-347 doi:10.1038/333345a0

Brillas E (2021) Recent development of electrochemical advanced oxidation of herbicides. A review on its application to wastewater treatment and soil remediation. Journal of Cleaner Production 290:125841 doi:https://doi.org/10.1016/j.jclepro.2021.125841

Buerge IJ, Bächli A, Kasteel R, et al. (2019) Behavior of the Chiral Herbicide Imazamox in Soils: pH-Dependent, Enantioselective Degradation, Formation and Degradation of Several Chiral Metabolites. Environmental Science & Technology 53(10):5725-5732 doi:10.1021/acs.est.8b07209

Bulut Y, Aydın H (2006) A kinetics and thermodynamics study of methylene blue adsorption on wheat shells. Desalination 194(1):259-267 doi:https://doi.org/10.1016/j.desal.2005.10.032

Buttiglieri G, Peschka M, Frömel T, et al. (2009) Environmental occurrence and degradation of the herbicide n-chloridazon. Water Research 43(11):2865-2873 doi:https://doi.org/10.1016/j.watres.2009.03.035

Calvet R (1989) Adsorption of organic chemicals in soils. Environmental Health Perspectives 83:145-177

Carballa M, Fink G, Omil F, Lema JM, Ternes T (2008) Determination of the solid–water distribution coefficient (Kd) for pharmaceuticals, estrogens and musk fragrances in digested sludge. Water Research 42(1):287-295 doi:https://doi.org/10.1016/j.watres.2007.07.012

Carneiro GDOP, Souza MdF, Lins HA, et al. (2020) Herbicide mixtures affect adsorption processes in soils under

sugarcane cultivation. Geoderma 379:114626 doi:https://doi.org/10.1016/j.geoderma.2020.114626

Cueff S, Alletto L, Dumény V, Benoit P, Pot V (2020) Adsorption and degradation of the herbicide nicosulfuron in a stagnic Luvisol and Vermic Umbrisol cultivated under conventional or conservation agriculture. Environmental Science and Pollution Research doi:10.1007/s11356-020-11772-2

de Matos AT, Fontes MPF, da Costa LM, Martinez MA (2001) Mobility of heavy metals as related to soil chemical and mineralogical characteristics of Brazilian soils. Environmental Pollution 111(3):429-435 doi:https://doi.org/10.1016/S0269-7491(00)00088-9

Fan X, Zou Y, Geng N, et al. (2021) Investigation on the adsorption and desorption behaviors of antibiotics by degradable MPs with or without UV ageing process. Journal of Hazardous Materials 401:123363 doi:https://doi.org/10.1016/j.jhazmat.2020.123363

FAO (2000) Assessing soil contamination A reference manual. FOOD AND AGRICULTURE ORGANIZATION OF THE UNITED NATIONS Rome, Rome

Gao H-J, Jiang X (2010) Effect of Initial Concentration on Adsorption-Desorption Characteristics and Desorption Hysteresis of Hexachlorobenzene in Soils. Pedosphere 20(1):104-110 doi:https://doi.org/10.1016/S1002-0160(09)60289-7

García-Delgado C, Marín-Benito JM, Sánchez-Martín MJ, Rodríguez-Cruz MS (2020) Organic carbon nature determines the capacity of organic amendments to adsorb pesticides in soil. Journal of Hazardous Materials 390:122162 doi:https://doi.org/10.1016/j.jhazmat.2020.122162

García-Valcárcel AI, Tadeo JL (1999) Influence of Soil Moisture on Sorption and Degradation of Hexazinone and Simazine in Soil. J Agric Food Chem 47(9):3895-3900 doi:10.1021/jf981326i

Gawel A, Seiwert B, Sühnholz S, Schmitt-Jansen M, Mackenzie K (2020) In-situ treatment of herbicide-contaminated groundwater–Feasibility study for the cases atrazine and bromacil using two novel nanoremediation-type materials. Journal of Hazardous Materials 393:122470 doi:https://doi.org/10.1016/j.jhazmat.2020.122470

GB (2014a) Test Guidelines of the Environmental Safety Assessment for Chemical Pesticides-Part 1 (Transformation in Soils) vol 31270.1-2014. China's General Administration of Quality Supervision, Inspection and Quarantine

GB (2014b) Test Guidelines of the Environmental Safety Assessment for Chemical Pesticides-Part 4: Adsorption/Desorption in Soils. China's General Administration of Quality Supervision, Inspection and Quarantine

GB (2014c) Test Guidelines on Environmental Safety Assessment for Chemical Pesticides: Part 5: Leaching in soil. vol GB/T 31270.5-2014,

Gee GW, and Bauder, J. W. (1986) 'Partcle-size analysis' in Methods of soil analysis, part-I. Physical and mineralogical methods,

Gustafson DI (1989) Groundwater ubiquity score: A simple method for assessing pesticide leachability. Environmental Toxicology and Chemistry 8(4):339-357 doi:10.1002/etc.5620080411

Hochman D, Dor M, Mishael Y (2021) Diverse effects of wetting and drying cycles on soil aggregation: Implications on pesticide leaching. Chemosphere 263:127910 doi:https://doi.org/10.1016/j.chemosphere.2020.127910

Huang B, Yan, D. D., Wang, X. N., Wang, X. L., Fang, W.S., Zhang, D. Q.,Ouyang, C. B., Wang, Qi. X., Cao, A. C. (2019) Soil fumigation alters adsorption and degradation behavior of pesticides in soil. Environmental Pollution 246:264-273 doi:https://doi.org/10.1016/j.envpol.2018.12.003

Inao K, Mizutani H, Yogo Y, Ikeda M (2009) Improved PADDY model including photoisomerization and metabolic

pathways for predicting pesticide behavior in paddy fields: Application to the herbicide pyriminobac-methyl. Journal of Pesticide Science advpub:0909190094-0909190094 doi:10.1584/jpestics.G09-20

Iwafune T, Inao K, Horio T, Iwasaki N, Yokoyama A, Nagai T (2010) Behavior of paddy pesticides and major metabolites in the Sakura River, Ibaraki, Japan. Journal of Pesticide Science advpub:1001130109-1001130109 doi:10.1584/jpestics.G09-49

Iwakami S, Hashimoto M, Matsushima K-i, Watanabe H, Hamamura K, Uchino A (2015) Multiple-herbicide resistance in Echinochloa crus-galli var. formosensis, an allohexaploid weed species, in dry-seeded rice. Pesticide Biochemistry and Physiology 119:1-8 doi:https://doi.org/10.1016/j.pestbp.2015.02.007

Jackson M (1958) Soil Chemical Analysis. prentice Hall. Inc, Englewood Cliffs, NJ,

Jia C-S, Zhang L-H, Peng X-L, et al. (2019) Prediction of entropy and Gibbs free energy for nitrogen. Chemical Engineering Science 202:70-74 doi:https://doi.org/10.1016/j.ces.2019.03.033

Jiang R, Wang M, Chen W, Li X (2018) Ecological risk evaluation of combined pollution of herbicide siduron and heavy metals in soils. Science of The Total Environment 626:1047-1056 doi:https://doi.org/10.1016/j.scitotenv.2018.01.135

Kalsi NK, Kaur P (2019) Dissipation of bispyribac sodium in aridisols: Impact of soil type, moisture and temperature. Ecotoxicology and Environmental Safety 170:375-382 doi:https://doi.org/10.1016/j.ecoenv.2018.12.005

Khan MA, Costa FB, Fenton O, Jordan P, Fennell C, Mellander P-E (2020) Using a multi-dimensional approach for catchment scale herbicide pollution assessments. Science of The Total Environment 747:141232 doi:https://doi.org/10.1016/j.scitotenv.2020.141232

Khorram MS, Sarmah AK, Yu Y (2018) The Effects of Biochar Properties on Fomesafen Adsorption-Desorption Capacity of Biochar-Amended Soil. Water, Air, & Soil Pollution 229(3):60 doi:10.1007/s11270-017-3603-2

Kulshrestha P, Giese RF, Aga DS (2004) Investigating the Molecular Interactions of Oxytetracycline in Clay and Organic Matter: Insights on Factors Affecting Its Mobility in Soil. Environmental Science & Technology 38(15):4097-4105 doi:10.1021/es034856q

L'Huillier L, Dupont, S., Dubus, I., Becquer, T., Bourdon, E., (1998) Carence et fixation du phosphore dans les sols ferrallitiques ferritiques de Nouvelle-Caledonie. Paper presented at the XVIe Congres Mondial de Science du Sol, Montpellier, France, 20-26

Lewis KA, Tzilivakis J, Warner DJ, Green A (2016) An international database for pesticide risk assessments and management. Human and Ecological Risk Assessment: An International Journal 22(4):1050-1064 doi:10.1080/10807039.2015.1133242

Liu J, Zhou JH, Guo QN, Ma LY, Yang H (2021) Physiochemical assessment of environmental behaviors of herbicide atrazine in soils associated with its degradation and bioavailability to weeds. Chemosphere 262:127830 doi:https://doi.org/10.1016/j.chemosphere.2020.127830

Marín-Benito JM, Carpio MJ, Sánchez-Martín MJ, Rodríguez-Cruz MS (2019) Previous degradation study of two herbicides to simulate their fate in a sandy loam soil: Effect of the temperature and the organic amendments. Science of The Total Environment 653:1301-1310 doi:https://doi.org/10.1016/j.scitotenv.2018.11.015

Martins EC, de Freitas Melo V, Bohone JB, Abate G (2018) Sorption and desorption of atrazine on soils: The effect of different soil fractions. Geoderma 322:131-139 doi:https://doi.org/10.1016/j.geoderma.2018.02.028

Martins JM, Mermoud A (1998) Sorption and degradation of four nitroaromatic herbicides in mono and multi-solute saturated/unsaturated soil batch systems. J Contam Hydrol 33(1):187-210 doi:https://doi.org/10.1016/S0169-7722(98)00070-9

Medo J, Hricáková N, Maková J, Medová J, Omelka R, Javoreková S (2020) Effects of sulfonylurea herbicides chlorsulfuron and sulfosulfuron on enzymatic activities and microbial communities in two agricultural soils. Environmental Science and Pollution Research 27(33):41265-41278 doi:10.1007/s11356-020-10063-0

Meimaroglou N, Mouzakis C (2019) Cation Exchange Capacity (CEC), texture, consistency and organic matter in soil assessment for earth construction: The case of earth mortars. Construction and Building Materials 221:27-39 doi:https://doi.org/10.1016/j.conbuildmat.2019.06.036

Nandi BK, Goswami A, Purkait MK (2009) Adsorption characteristics of brilliant green dye on kaolin. Journal of Hazardous Materials 161(1):387-395 doi:https://doi.org/10.1016/j.jhazmat.2008.03.110

Nelson D, Sommers, L., (1985) Total carbon, organic carbon and organic matter. . American Society of Agronomy, USA

Obregón Alvarez D, Mendes KF, Tosi M, et al. (2021) Sorption-desorption and biodegradation of sulfometuron-methyl and its effects on the bacterial communities in Amazonian soils amended with aged biochar. Ecotoxicology and Environmental Safety 207:111222 doi:https://doi.org/10.1016/j.ecoenv.2020.111222

Ou J, Li H, Ou X, et al. (2020) Degradation, adsorption and leaching of phenazine-1-carboxamide in agricultural soils. Ecotoxicology and Environmental Safety 205:111374 doi:https://doi.org/10.1016/j.ecoenv.2020.111374

Patel KF, Tejnecký V, Ohno T, Bailey VL, Sleighter RL, Hatcher PG (2021) Reactive oxygen species alter chemical composition and adsorptive fractionation of soil-derived organic matter. Geoderma 384:114805 doi:https://doi.org/10.1016/j.geoderma.2020.114805

Pérez-Lucas G, Gambín M, Navarro S (2020) Leaching behaviour appraisal of eight persistent herbicides on a loam soil amended with different composted organic wastes using screening indices. Journal of Environmental Management 273:111179 doi:https://doi.org/10.1016/j.jenvman.2020.111179

Perotti VE, Larran AS, Palmieri VE, Martinatto AK, Permingeat HR (2020) Herbicide resistant weeds: A call to integrate conventional agricultural practices, molecular biology knowledge and new technologies. Plant Science 290:110255 doi:https://doi.org/10.1016/j.plantsci.2019.110255

Qin M, Chai S, Ma Y, Gao H, Zhang H, He Q (2017) Determination of pyriminobac-methyl and bispyribac-sodium residues in rice by liquid chromatography-tandem mass spectrometry based on QuEChERS. Se pu = Chinese journal of chromatography 35(7):719-723 doi:10.3724/sp.J.1123.2017.02032

Rae JE, Cooper CS, Parker A, Peters A (1998) Pesticide sorption onto aquifer sediments. Journal of Geochemical Exploration 64(1):263-276 doi:https://doi.org/10.1016/S0375-6742(98)00037-5

Rao L, Luo J, Zhou W, Zou Z, Tang L, Li B (2020) Adsorption–desorption behavior of benzobicyclon hydrolysate in different agricultural soils in China. Ecotoxicology and Environmental Safety 202:110915 doi:https://doi.org/10.1016/j.ecoenv.2020.110915

Shibayama H (2001) Weeds and weed management in rice production in Japan. Weed Biology and Management 1(1):53-60 doi:https://doi.org/10.1046/j.1445-6664.2001.00004.x

Silva TS, de Freitas Souza M, Maria da Silva Teófilo T, et al. (2019) Use of neural networks to estimate the sorption and desorption coefficients of herbicides: A case study of diuron, hexazinone, and sulfometuron-methyl in Brazil. Chemosphere 236:124333

doi:https://doi.org/10.1016/j.chemosphere.2019.07.064

Song H, Mao H, Shi D (2010) Synthesis and Herbicidal Activity of α-Hydroxy Phosphonate Derivatives Containing Pyrimidine Moiety. 28(10):2020-2024 doi:https://doi.org/10.1002/cjoc.201090337

Spadotto CA, Locke MA, Bingner RL, Mingoti R (2020) Estimating sorption of monovalent acidic herbicides at different pH levels using a single sorption coefficient. Pest Management Science 76(8):2693-2698 doi:https://doi.org/10.1002/ps.5815

Sudo M, Goto Y, Iwama K, Hida Y (2018) Herbicide discharge from rice paddy fields by surface runoff and percolation flow: A case study in paddy fields in the Lake Biwa basin, Japan. Journal of Pesticide Science 43(1):24-32 doi:10.1584/jpestics.D17-061

Tamaru M, Masuyama N, Sato M, Takabe F, Inoue J, Hanai R (1997) Studies of the New Herbicide KIH-6127. Part III. Synthesis and Structure–Activity Studies of Analogues of KIH-6127 against Barnyard Grass (Echinochloa oryzicola)*. Pesticide Science 49(1):76-84 doi:https://doi.org/10.1002/(SICI)1096-9063(199701)49:1<76::AID-PS491>3.0.CO;2-E

Tamaru M, Saito Y (1996) Studies of the New Herbicide KIH-6127. Part I. Novel Synthesis of Methyl 6-Acetylsalicylate as a Key Synthetic Intermediate for the Preparation of 6-Acetyl Pyrimidin-2-yl Salicylates and Analogues. Pesticide Science 47(2):125-130 doi:https://doi.org/10.1002/(SICI)1096-9063(199606)47:2<125::AID-PS394>3.0.CO;2-X

Tang W, Yu Z-H, Shi D-Q (2010) Synthesis, crystal structure, and herbicidal activity of pyrimidinyl benzylamine analogues containing a phosphonyl group. Heteroatom Chemistry 21(3):148-155 doi:https://doi.org/10.1002/hc.20589

Temminghoff EJM, Van der Zee SEATM, de Haan FAM (1997) Copper Mobility in a Copper-Contaminated Sandy Soil as Affected by pH and Solid and Dissolved Organic Matter. Environmental Science & Technology 31(4):1109-1115 doi:10.1021/es9606236

Ternes TA, Herrmann N, Bonerz M, Knacker T, Siegrist H, Joss A (2004) A rapid method to measure the solid–water distribution coefficient (Kd) for pharmaceuticals and musk fragrances in sewage sludge. Water Research 38(19):4075-4084 doi:https://doi.org/10.1016/j.watres.2004.07.015

Urach Ferreira PH, Ferguson JC, Reynolds DB, Kruger GR, Irby JT (2020) Droplet size and physicochemical property effects on herbicide efficacy of pre-emergence herbicides in soybean (Glycine max (L.) Merr). 76(2):737-746 doi:https://doi.org/10.1002/ps.5573

Wang HZ, Zuo HG, Ding YJ, Miao SS, Jiang C, Yang H (2014) Biotic and abiotic degradation of pesticide Dufulin in soils. Environmental Science and Pollution Research 21(6):4331-4342 doi:10.1007/s11356-013-2380-8

Wang Q, Fu Y, Zhang l, Ling S, Wu Y (2020a) Determination of pyriminobac-methyl isomers in paddy and its storage stability. Journal of Food Safety and Quality 20(11):7429-7435

Wang Z, Yang L, Cheng P, Yu Y, Zhang Z, Li H (2020b) Adsorption, degradation and leaching migration characteristics of chlorothalonil in different soils. European Journal of Remote Sensing:1-10 doi:10.1080/22797254.2020.1771216

Wei L, Huang Y, Huang L, et al. (2020) The ratio of H/C is a useful parameter to predict adsorption of the herbicide metolachlor to biochars. Environmental Research 184:109324 doi:https://doi.org/10.1016/j.envres.2020.109324

Wu X, Wang W, Liu J, et al. (2017) Rapid Biodegradation of the Herbicide 2,4-Dichlorophenoxyacetic Acid by Cupriavidus gilardii T-1. J Agric Food Chem 65(18):3711-3720 doi:10.1021/acs.jafc.7b00544

Xiang L, Wang, X. D., Chen, X. H., Mo, C. H., Li, Y. W., Li, H., Cai, Q. Y., Zhou, D. M., Wong, M. H., Li, Q. X. (2019) Sorption Mechanism, Kinetics, and Isotherms of Di-n-butyl Phthalate to Different Soil Particle-Size

Fractions. J Agric Food Chem 67(17):4734-4745 doi:10.1021/acs.jafc.8b06357

Xie G, Li B, Tang L, Rao L, Dong Z (2020) Adsorption-desorption and leaching behaviors of broflanilide in four texturally different agricultural soils from China. Journal of Soils and Sediments doi:10.1007/s11368-020-02831-9

Xu Y, Liu J, Cai W, et al. (2020) Dynamic processes in conjunction with microbial response to disclose the biochar effect on pentachlorophenol degradation under both aerobic and anaerobic conditions. Journal of Hazardous Materials 384:121503 doi:https://doi.org/10.1016/j.jhazmat.2019.121503

Xu Y, Yu X, Xu B, Peng D, Guo X (2021) Sorption of pharmaceuticals and personal care products on soil and soil components: Influencing factors and mechanisms. Science of The Total Environment 753:141891 doi:https://doi.org/10.1016/j.scitotenv.2020.141891

Yang R, Jia A, He S, et al. (2021) Experimental investigation of water vapor adsorption isotherm on gas-producing Longmaxi shale: Mathematical modeling and implication for water distribution in shale reservoirs. Chemical Engineering Journal 406:125982 doi:https://doi.org/10.1016/j.cej.2020.125982

Yin X, Zelenay P (2018) (Invited)Kinetic Models for the Degradation Mechanisms of PGM-Free ORR Catalysts. ECS Transactions 85(13):1239-1250 doi:10.1149/08513.1239ecst

Yoshii K, Okada M, Tsumura Y, Nakamura Y, Ishimttsu S, Tonogai Y (2020) Supercritical Fluid Extraction of Ten Chloracetanilide Pesticides and Pyriminobac-Methyl in Crops: Comparison with the Japanese Bulletin Method. Journal of AOAC INTERNATIONAL 82(5):1239-1245 doi:10.1093/jaoac/82.5.1239 %J Journal of AOAC INTERNATIONAL

Yu Y, Zhuang Y-Y, Wang Z-H, Qiu M-Q (2004) Adsorption of water-soluble dyes onto modified resin. Chemosphere 54(3):425-430 doi:https://doi.org/10.1016/S0045-6535(03)00654-4

Yue L, Ge C, Feng D, Yu H, Deng H, Fu B (2017) Adsorption–desorption behavior of atrazine on agricultural soils in China. Journal of Environmental Sciences 7(57):180-189

Zhang C-L, Qiao G-L, Zhao F, Wang Y (2011) Thermodynamic and kinetic parameters of ciprofloxacin adsorption onto modified coal fly ash from aqueous solution. Journal of Molecular Liquids 163(1):53-56 doi:https://doi.org/10.1016/j.molliq.2011.07.005

Zhang S, Han B, Sun Y, Wang F (2020a) Microplastics influence the adsorption and desorption characteristics of Cd in an agricultural soil. Journal of Hazardous Materials 388:121775 doi:https://doi.org/10.1016/j.jhazmat.2019.121775

Zhang Y, Li W, Zhou W, Jia H, Li B (2020b) Adsorption-desorption characteristics of pyraclonil in eight agricultural soils. Journal of Soils and Sediments 20(3):1404-1412 doi:10.1007/s11368-019-02471-8

Zhou W, Zhang Y, Li W, Jia H, Huang H, Li B (2019a) Adsorption isotherms, degradation kinetics, and leaching behaviors of cyanogen and hydrogen cyanide in eight texturally different agricultural soils from China. Ecotoxicology and Environmental Safety 185:109704 doi:https://doi.org/10.1016/j.ecoenv.2019.109704

Zhou Z, Yan T, Zhu Q, et al. (2019b) Bacterial community structure shifts induced by biochar amendment to karst calcareous soil in southwestern areas of China. Journal of Soils and Sediments 19(1):356-365 doi:10.1007/s11368-018-2035-y

**Table 1**

Comparison between the results of the linear and Freundlich models for the adsorption–desorption of EPM in five agricultural soils.

| Soil sample | Soil type | Adsorption | | | | | | Desorption | | | | | |
|---|---|---|---|---|---|---|---|---|---|---|---|---|---|
| | | Linear model | | | Freundlich model | | | Linear model | | Freundlich model | | | |
| | | $K$ (mL g$^{-1}$) [a] | $C_0$ (mg kg$^{-1}$) [a] | $R^2$ | $K_{f\text{-}ads}$ (mg$^{1-1/n}$ L$^{1/n}$ kg$^{-1}$) [a] | $1/n_{ads}$ [a] | $R^2$ | $K$ (mL g$^{-1}$) [a] | $R^2$ | $K_{f\text{-}des}$ (mg$^{1-1/n}$ L$^{1/n}$ kg$^{-1}$) [a] | $1/n_{des}$ [a] | $R^2$ | $H$ |
| S1 | Phaeozem | 56.21 ± 3.56 | 0.17 ± 0.01 | 0.9841 | 32.22 ± 4.55 | 0.80 ± 0.07 | 0.9999 | 0.80 ± 0.24 | 0.8384 | 5.02 ± 0.02 | 0.01 ± 33.53 | 0.9999 | 0.013 |
| S2 | Anthrosol | 2.78 ± 0.06 | 0.13 ± 0.04 | 0.9982 | 2.95 ± 0.04 | 0.88 ± 0.03 | 0.9999 | 0.27 ± 0.03 | 0.9823 | 2.27 ± 0.01 | 0.71 ± 0.28 | 0.9999 | 0.807 |
| S3 | Ferralsol | 2.43 ± 0.07 | 0.16 ± 0.05 | 0.9975 | 2.65 ± 0.03 | 0.84 ± 0.03 | 0.9999 | 0.82 ± 0.19 | 0.8988 | 1.73 ± 0.05 | 0.11 ± 1.43 | 0.9999 | 0.131 |
| S4 | Alisol | 0.79 ± 0.01 | 0.05 ± 0.01 | 0.9990 | 0.85 ± 0.02 | 0.95 ± 0.03 | 0.9999 | 0.53 ± 0.05 | 0.9834 | 0.78 ± 0.01 | 0.12 ± 0.01 | 1.0000 | 0.126 |
| S5 | Plinthosol | 2.03 ± 0.07 | −0.01 ± 0.06 | 0.9951 | 1.99 ± 0.05 | 1.06 ± 0.04 | 0.9999 | 2.53 ± 0.18 | 0.9905 | 1.38 ± 0.08 | 0.19 ± 0.56 | 0.9999 | 0.179 |

[a] The values represent means ± standard error (SE, n = 3).

**Table 2**

Empirical constants, Gibbs free energy, and groundwater ubiquity score (GUS) for the adsorption of EPM in five agricultural soils.

| Soil sample | Soil type | K | $C_e/C_0$ | $K_{f\text{-}ads}$ ($mg^{1-1/n}$ $L^{1/n}$ $kg^{-1}$) | $K_{OC}$ | $K_{OM}$ | △G (kJ $mol^{-1}$) | GUS |
|---|---|---|---|---|---|---|---|---|
| S1 | Phaeozem | 64.4821 | 0.0117 | 32.2230 | 2395.8435 | 695.6897 | −16.2242 | 0.9765 |
| S2 | Anthrosol | 3.0971 | 0.2441 | 2.9540 | 606.7513 | 335.2273 | −14.4143 | 2.0402 |
| S3 | Ferralsol | 2.7861 | 0.2641 | 2.6530 | 289.3500 | 159.6386 | −12.5753 | 2.7160 |
| S4 | Alisol | 0.8393 | 0.5437 | 0.8520 | 413.3906 | 242.8571 | −13.6153 | 2.3755 |
| S5 | Plinthosol | 2.0172 | 0.3314 | 1.9950 | 289.8034 | 165.8333 | −12.6696 | 2.6765 |

**Table 3**

Degradation kinetic models and parameters of EPM under different conditions.

| Soil sample | Soil type | Aerobic | | | Anaerobic | | | Sterilized | | |
|---|---|---|---|---|---|---|---|---|---|---|
| | | First-order kinetic model | Half-life $t_{1/2}$ (d) | $R^2$ | First-order kinetic model | Half- life $t_{1/2}$ (d) | $R^2$ | First-order kinetic model | Half- life $t_{1/2}$ (d) | $R^2$ |
| S1 | Phaeozem | $C_t = 1.5338e^{-0.0185t}$ | 37.46 | 0.9473 | $C_t = 1.7792e^{-0.0166t}$ | 41.75 | 0.9579 | $C_t = 1.8467e^{-0.0111t}$ | 62.43 | 0.9800 |
| S2 | Anthrosol | $C_t = 1.6419e^{-0.0146t}$ | 47.47 | 0.9707 | $C_t = 1.8599e^{-0.0139t}$ | 49.85 | 0.9696 | $C_t = 1.7543e^{-0.0113t}$ | 60.87 | 0.9551 |
| S3 | Ferralsol | $C_t = 1.9363e^{-0.0119t}$ | 58.25 | 0.9843 | $C_t = 1.9968e^{-0.0116t}$ | 59.74 | 0.9878 | $C_t = 1.9349e^{-0.0105t}$ | 66.00 | 0.9775 |
| S4 | Alisol | $C_t = 1.9476e^{-0.0133t}$ | 52.10 | 0.9924 | $C_t = 1.9477e^{-0.0133t}$ | 52.11 | 0.9924 | $C_t = 1.7086e^{-0.0112t}$ | 61.88 | 0.9313 |
| S5 | Plinthosol | $C_t = 1.7864e^{-0.0126t}$ | 55.00 | 0.9655 | $C_t = 1.9725e^{-0.0121t}$ | 57.27 | 0.9923 | $C_t = 1.8638e^{-0.0109t}$ | 63.58 | 0.9761 |

**Table 4**

Degradation kinetic models and parameters of EPM in soil under different moisture conditions.

| Soil sample | Soil type[a] | Saturation moisture capacity (40%) | | | Saturation moisture capacity (60%) | | | Saturation moisture capacity (80%) | | |
|---|---|---|---|---|---|---|---|---|---|---|
| | | First-order kinetic model | Half-life $t_{1/2}$ (d) | $R^2$ | First-order kinetic model | Half-life $t_{1/2}$ (d) | $R^2$ | First-order kinetic model | Half-life $t_{1/2}$ (d) | $R^2$ |
| S1 | Phaeozem | $C_t = 1.7324e^{-0.0141t}$ | 49.15 | 0.9582 | $C_t = 1.5338e^{-0.0185t}$ | 37.46 | 0.9473 | $C_t = 1.7792e^{-0.0166t}$ | 41.75 | 0.9579 |
| S2 | Anthrosol | $C_t = 1.6551e^{-0.0133t}$ | 52.11 | 0.8769 | $C_t = 1.6419e^{-0.0146t}$ | 47.47 | 0.9707 | $C_t = 1.8599e^{-0.0139t}$ | 49.87 | 0.9696 |
| S3 | Ferralsol | $C_t = 1.8659e^{-0.0110t}$ | 62.77 | 0.9884 | $C_t = 1.9363e^{-0.0119t}$ | 58.25 | 0.9843 | $C_t = 1.9968e^{-0.0116t}$ | 59.74 | 0.9878 |
| S4 | Alisol | $C_t = 1.8428e^{-0.0116t}$ | 59.74 | 0.9742 | $C_t = 1.9476e^{-0.0133t}$ | 52.10 | 0.9924 | $C_t = 1.7076e^{-0.0121t}$ | 57.27 | 0.9849 |
| S5 | Plinthosol | $C_t = 1.7637e^{-0.0104t}$ | 66.63 | 0.9650 | $C_t = 1.7864e^{-0.0126t}$ | 55.00 | 0.9655 | $C_t = 1.9725e^{-0.0121t}$ | 57.27 | 0.9923 |

Figure legends:

**Fig. 1.** Adsorption (a) and desorption (b) kinetic curves and Adsorption (c) and desorption (d) isothermal curves of EPM in five different agricultural soils (S1 to S5 are defined in Table 1). Values are the means ± standard error (n=3).

**Fig. 2.** Degradation kinetics of EPM under aerobic (a), anaerobic (b), sterilization (c) conditions with 60% moisture, under aerobic conditions with 40% moisture(d) and with 80% moisture(e)in five different agricultural soils (S1 to S5 are defined in Table 1). Values are the means ± standard error (n=3).

**Fig. 3.** Distribution of EPM in soil column and leachate of five different agricultural soils (S1 to S5 are defined in Table 1)

# Figures

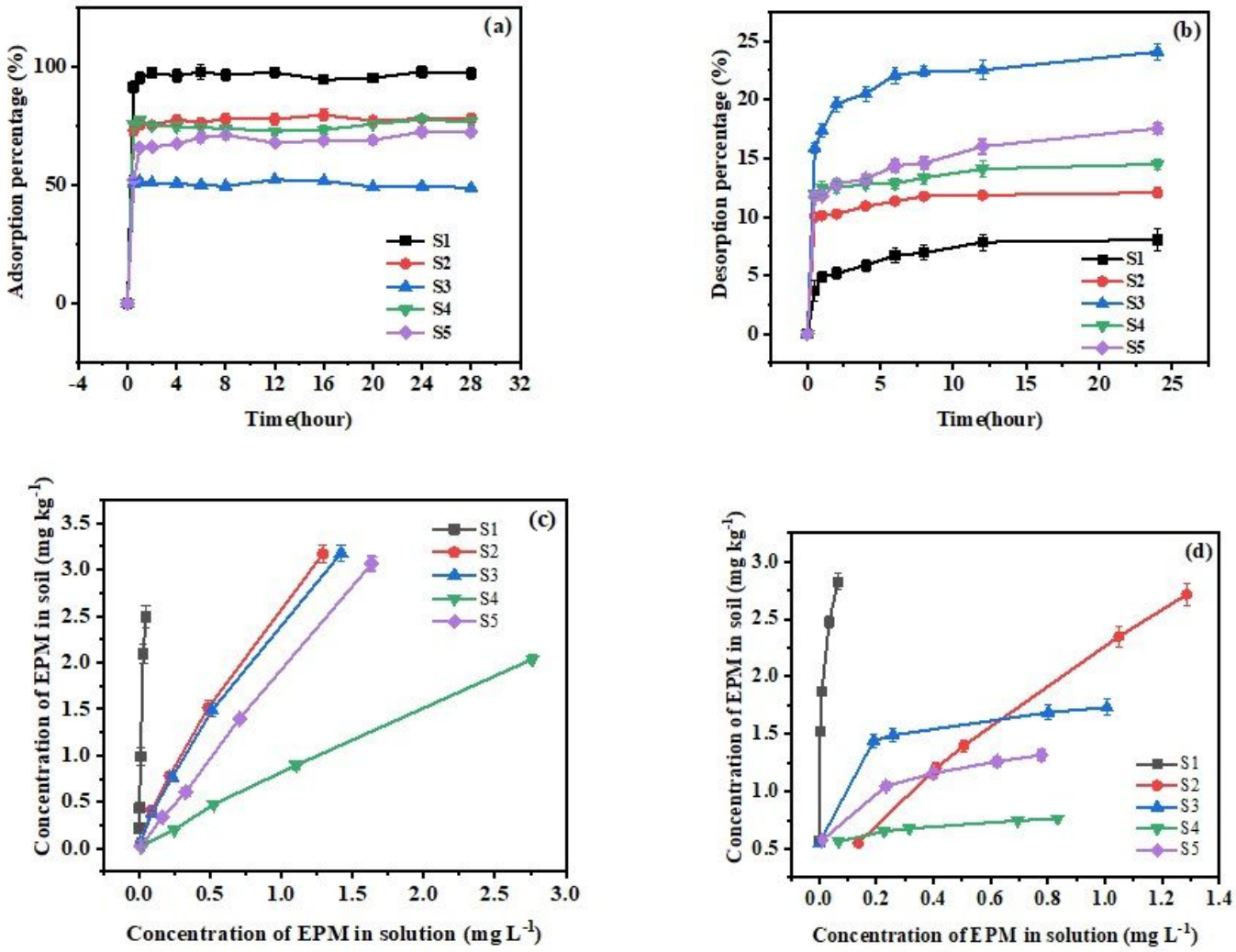


## Figure 1

Adsorption (a) and desorption (b) kinetic curves and Adsorption (c) and desorption (d) isothermal curves of EPM in five different agricultural soils (S1 to S5 are defined in Table 1). Values are the means ± standard error (n=3).

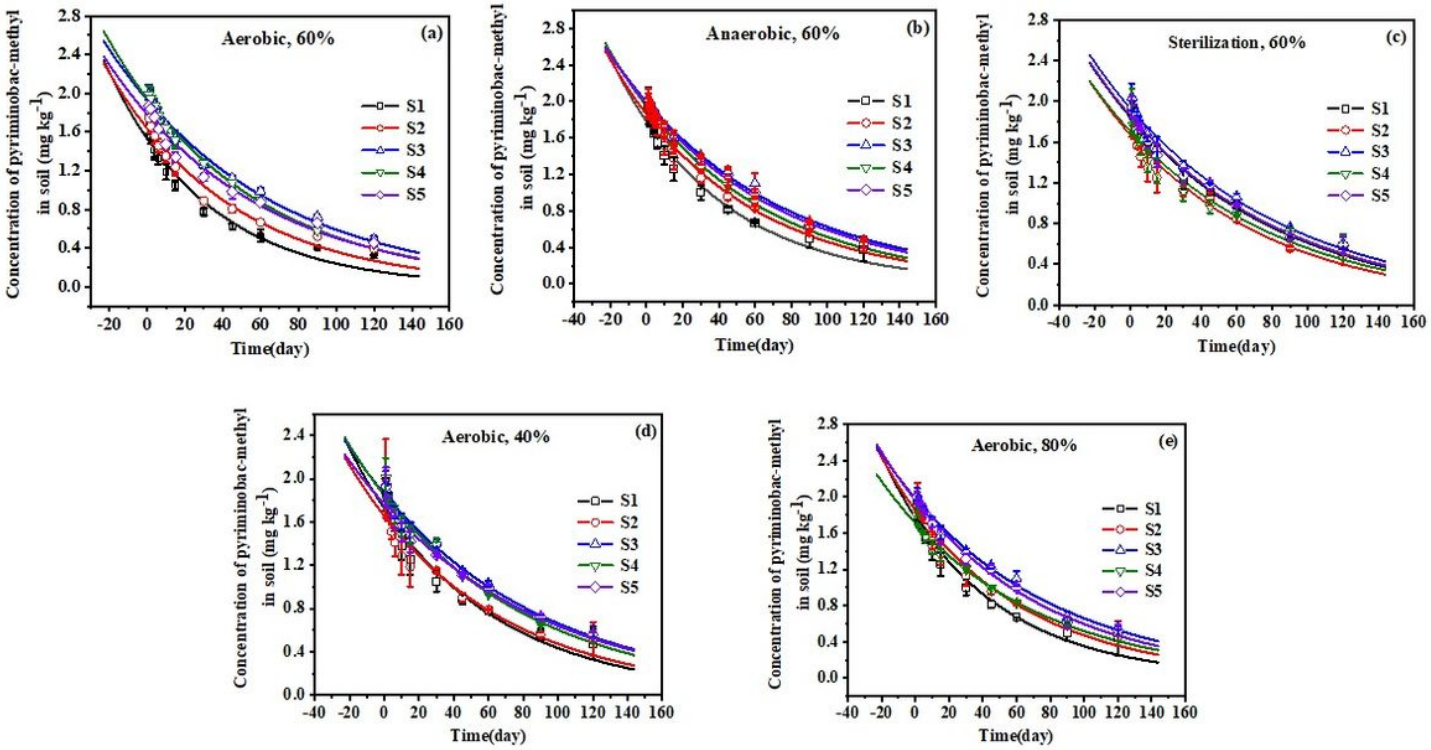


## Figure 2

Degradation kinetics of EPM under aerobic (a), anaerobic (b), sterilization (c) conditions with 60% moisture, under aerobic conditions with 40% moisture(d) and with 80% moisture(e)in five different agricultural soils (S1 to S5 are defined in Table 1). Values are the means ± standard error (n=3).

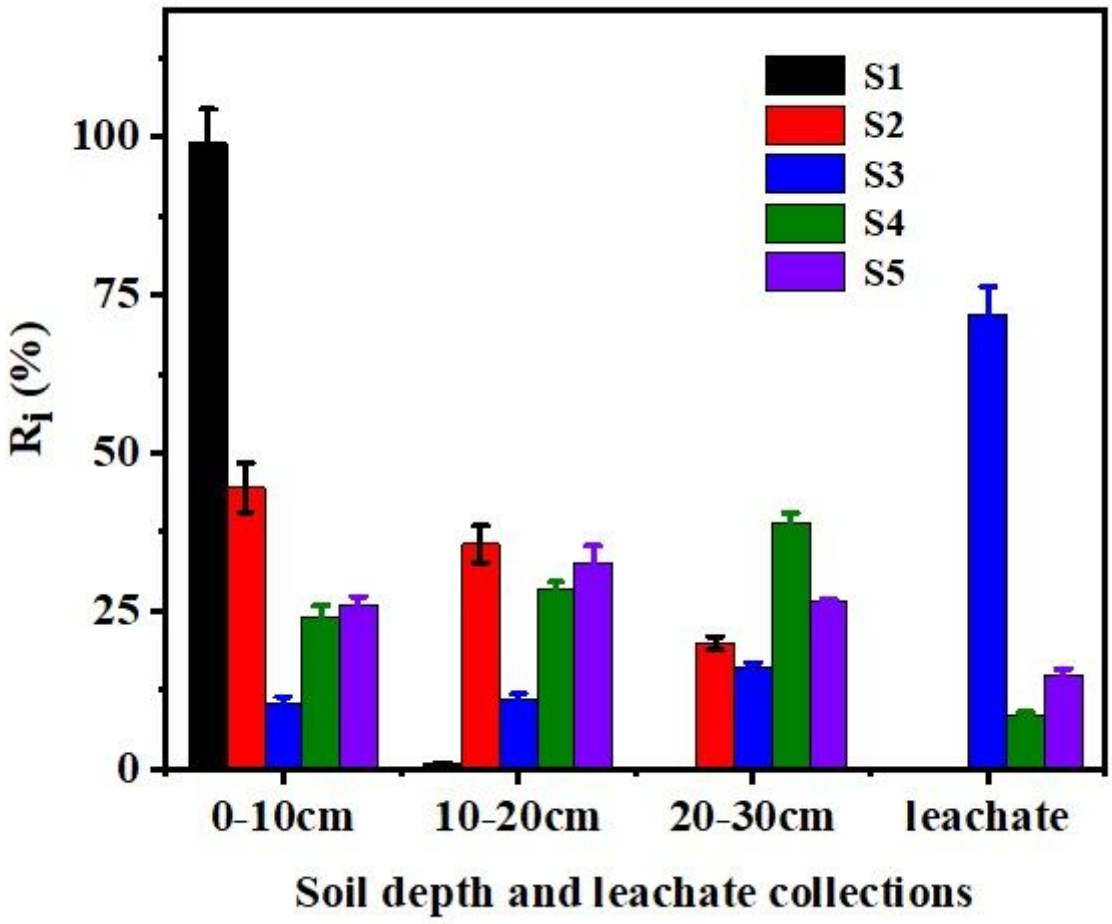


**Figure 3**

Distribution of EPM in soil column and leachate of five different agricultural soils (S1 to S5 are defined in Table 1)

## Supplementary Files

This is a list of supplementary files associated with this preprint. Click to download.

- Supplementarymaterial.doc